Study of Plasma Rotation in GOL-3 Multiple-Mirror Trap

V.V. Postupaev[1,2], A.V. Burdakov[1,2], I.A. Ivanov[1,2], K.I. Mekler[1], A.F. Rovenskikh[1], S.V. Polosatkin[1,3], S.L. Sinitsky[1,2], N.V. Sorokina[1], A.V. Sudnikov[1]

[1]*Budker Institute of Nuclear Physics SB RAS, Novosibirsk 630090, Russia*

[2]*Novosibirsk State University, Novosibirsk 630090, Russia*

[3]*Novosibirsk State Technical University, Novosibirsk 630092, Russia*

1. INTRODUCTION

The study of plasma rotation is of current interest for various magnetic confinement systems. The aim of this work is to analyze the rotation velocity in the GOL-3 multimirror trap [1]. When a high-current relativistic electron beam is used for fast collective heating of plasma in the GOL-3 facility, the properties of the plasma change sharply at transition from the beam heating stage to the confinement stage. At the heating stage, the beam excites small-scale Langmuir turbulence in the plasma. In this turbulent plasma, a specific radial structure of the longitudinal current appears and forms an azimuthal magnetic field with strong shear [2]. At the cooling stage, the mentioned current structure creating the azimuthal magnetic field holds for a certain time and, then, decays gradually as the plasma is cooled.

There are only the data obtained in [3] from chord measurements of the luminosity of the plasma in the VUV range at a plasma density of $(0.7\text{-}0.8)\times10^{21}$ m^{-3}. The structures corresponding to the modes with the azimuthal numbers $m = 2$ and 6 were observed.

In this work, we used two diagnostics: an array of Mirnov coils and a CCD camera operating in the slit scan regime at 2.5×10^5 fps. More details including mathematical procedures employed will be published in [4].

2. FACILITY AND OPERATING REGIMES

The device itself is an 11-m-long solenoid with axially-periodical (corrugated) magnetic field [1]. In the basic operation regime the solenoid consists of 52 magnetic corrugation cells with B_{max}/B_{min} = 4.8/3.2 T (the mirror ratio R = 1.5). Deuterium plasma of $10^{20}\div10^{22}$ m^{-3} density is heated up to ~2 keV ion temperature (at $\sim10^{21}$ m^{-3} density and $\tau_E \sim 1$ ms) by a high power relativistic electron beam. Typical beam parameters in the standard configuration are ~0.8 MeV, ~20 kA, ~12 μs, ~120 kJ.

Below, we discuss the results obtained in shots PL10630 and PL10647 that are considered as typical of regimes with low and high plasma densities. In the former shot, a bell-shaped

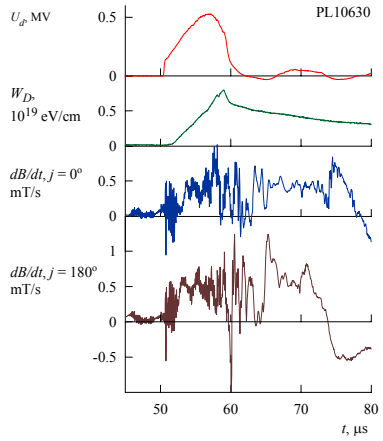

Fig. 1. Waveforms for typical shot no. PL10630. The voltage on the beam generator diode U_d, diamagnetic energy W_d at z = 264 cm, and signals from two Mirnov coils at angles of 0° and 180° are shown from top to bottom.

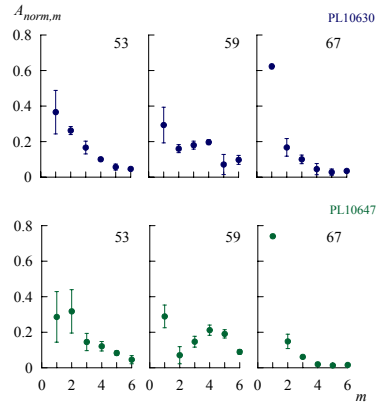

Fig. 2. Normalized amplitudes of the first azimuthal modes in 3, 9, and 17 μs after the beginning of electron beam injection.

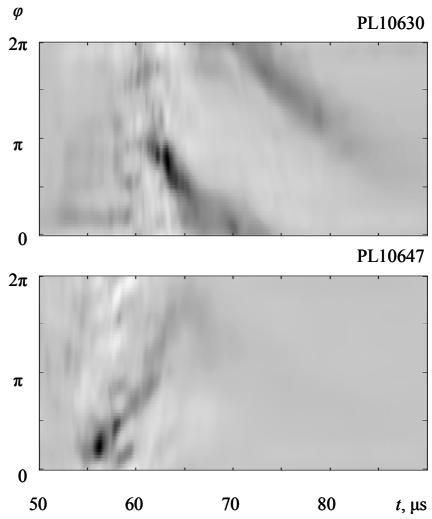

Fig. 3. Distortion of the magnetic surface.

longitudinal distribution of the D_2 with a maximum of $n_c = 1.6\times10^{21}$ m^{-3} was created. In PL10647, the central density was $n_c = 0.45\times10^{21}$ m^{-3}, but an additional 1-m-long bunch with $n_{max} \sim 3\times10^{21}$ m^{-3} was formed near the coordinate z = 1.15 m. Here we characterize the facility operation regime by the initial deuterium density n_0 measured at z = 83 cm in the maximum energy release region. The density is $n_0 = 7\times10^{20}$ and 2.6×10^{21} m^{-3} for shots PL10630 and PL10647.

3. EXPERIMENTAL RESULTS

Typical waveforms including signals of two Mirnov channels spaced by 180° are shown in Fig. 1. The beam injection starts at t = 50 μs. The frequency spectrum was analyzed in detail in [5]; here, we focus on the dynamics of distortions of the magnetic surface. The m = 1 dominates at the heating stage. For higher modes, the spectrum evolves toward smaller scale with a characteristic time of ~5 μs; i.e., the maximum shifts gradually from m = 2 to m = 5-6, which are the maximum m values resolved by our measuring system. Figure 2 shows the spatial spectra at several moments.

Expected rotation velocity of the plasma owing to $\boldsymbol{E}\times\boldsymbol{B}$ drift can be estimated as $\omega \sim 10^5$ s^{-1}. Typical results are presented in Fig. 3, which shows maps of magnetic perturbations for two shots; black color grades 0 and 255 (maximum negative and positive displacements) correspond to $\Delta r \approx 4$ mm. The amplitudes and phases are shown in Fig. 4.

At a high n_0 (Figs. 3a, 4a), the distortion increases during electron beam injection. In this case, the rotation of the first two modes occurs with a low angular velocity in the direction corresponding to $\boldsymbol{E}\times\boldsymbol{B}$ drift at a negative plasma potential. Then, after the termination of the beam injection, the rotation direction changes

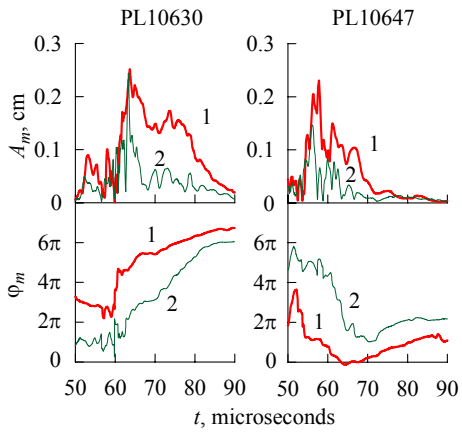

Fig. 4. Time dependences of the amplitude A_m and phase φ_m for the (1) first and (2) second azimuthal modes.

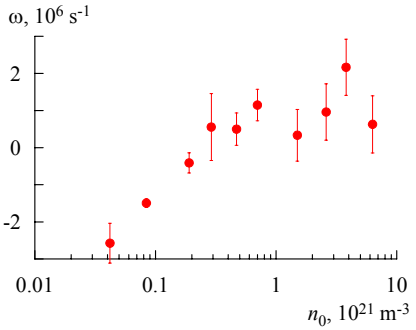

Fig. 5. Angular velocity of the rotation of the current boundary of the plasma vs. n_0.

and its angular velocity is ~3×10^5 s^{-1}. Until the termination of certainly detected signals, the plasma rotates in the expected direction corresponding to a positive ambipolar potential of the plasma.

At a low $n_0 < 2\times10^{20}$ m^{-3}, the situation changes strongly (Figs. 3b, 4b). The amplitude of the first two modes increases more rapidly, and the angular frequency of the plasma increases to ~10^6 s^{-1} in the direction corresponding to a negative potential. Rotation in this direction continues for a noticeable time (to 15-25 μs) after the termination of electron beam injection. Further, as in the case of a high density, the direction of the rotation of magnetic perturbations changes and coincides with the direction of $\boldsymbol{E}\times\boldsymbol{B}$ drift at the positive ambipolar potential of the plasma.

The observed rotation of m = 1 and 2 modes can be different, and even the opposite rotation directions of perturbations with different modes are sometimes observed (see, e.g., the interval of 63-67 μs in Fig. 4b). This can be due to different radial localization of these perturbations.

The periphery of the plasma, which emits in the optical range, rotates for most time with an angular velocity of about 5×10^4 s^{-1}. At the same time the rotation velocity of the paraxial region of the plasma is much lower. Thus, during and immediately after the injection of the relativistic electron beam, the shear rotation of the plasma is possible, which is characterized by the relative shift of different layers at an angle up to 4π.

The rotation direction and velocity of the plasma are shown in Fig. 5 as functions of the initial density of deuterium in the trap. This figure shows the average angular rotation velocity of magnetic perturbations calculated for 12.5 μs from the beginning of electron beam injection. As can be seen in the figure, at densities of about 3×10^{20} m^{-3} or higher, the initial rotation velocity is almost independent of the density (taking into account the indicated statistical error of the measurements). At the same time, at densities below 2×10^{20} m^{-3}, the average angular rotation velocity first changes sign and, then, increases to about 2×10^6 s^{-1}. The cooling of the plasma is accompanied by a decrease in the observed angular rotation frequency of the outer layer of the plasma, which rotates during the experiment by an angle of up to 4π.

4. DISCUSSION AND SUMMARY

In the experiments on plasma heating by the relativistic electron beam in GOL-3, plasma rotation has been revealed. The rotation velocity corresponds to the $\boldsymbol{E}\times\boldsymbol{B}$ drift at the electric field corresponding to $T_e \sim 1$ keV. In the experiments with the low-density plasma, plasma rotation in the opposite direction has been observed in 15-25 μs after the beginning of the beam injection. Signs of the differential rotation of the plasma have also been revealed.

The ratio of the electron density in the relativistic beam to the electron density in the plasma is about 10^{-4}-10^{-3}. Thus the injection of an additional charge can be easily compensated by longitudinal currents. The direct introduction of the potential in the presence of an electric contact of the plasma with biased end electrodes could also be proposed, but is not compatible with the dependence on density.

The known density dependence of the beam-plasma interaction efficiency can be a possible reason for the appearance of a negative potential. With an increase in the beam/plasma density ratio the anomalous electron collision frequency (see, e.g., [6]) can increase in the resistivity of the plasma to values at which the longitudinal current leads to the appearance of the observed potential even in a quite hot plasma. Another possible consequence of a more intense beam-plasma interaction at low densities can be stronger scattering and capture of relativistic electrons. Such a mechanism can exist, but even with optimistic estimates of the ratio of the densities of the plasma and captured electrons is much smaller than unity; consequently, the plasma can easily ensure the required compensating current.

More definite analysis of the reasons for a change in the sign of rotation at beam injection into the low-density plasma requires additional experimental data.

ACKNOWLEDGMENTS

This work was financially supported in part by the Ministry of Education and Science of the Russian Federation, by the Russian Government project no. 11.G34.31.0033, the Presidium of the Russian Academy of Sciences program no. 30, the Council of the Russian Presidential Grants project no. NSh-7792.2010.2, the RFBR projects 10-02-01317-a, 11-01-00249-a and 11-02-00563-a, the Dynasty Foundation, and Novosibirsk mayor's office.

References

1. A. Burdakov, A. Arzhannikov, V. Astrelin, et al., Fusion Sci. Technol., **55** (2T), 63 (2009).
2. V.V. Postupaev, A.V. Arzhannikov, V.T. Astrelin, et al., Fusion Sci. Technol., **47** (1T), 84 (2005).
3. V.V. Postupaev, et al., in Proc. 30th EPS Plasma Phys. Conf., St. Petersburg, ECA **27A**, P-2.193 (2003).
4. A.V. Sudnikov, A.V. Burdakov, I.A. Ivanov, et al., *accepted to* Plasma Physics Reports, **38** (2012).
5. V.V. Postupaev and A.V. Sudnikov, Vestnik NGU, Ser. Fizika, **2** (3), 62 (2007). – *in Russian*
6. A.V. Arzhannikov, V.T. Astrelin, A.V. Burdakov, et al., Fusion Technol., **35**, 223 (1999).